Conserved fungal effector suppresses PAMP-triggered immunity by targeting plant immune kinases

Hiroki Irieda[a,b], Yoshihiro Inoue[a], Masashi Mori[c], Kohji Yamada[a,d], Yuu Oshikawa[c], Hiromasa Saitoh[e,f], Aiko Uemura[f], Ryohei Terauchi[a,f], Saeko Kitakura[a], Ayumi Kosaka[a], Suthitar Singkaravanit-Ogawa[a], and Yoshitaka Takano[a,1]

[a]Graduate School of Agriculture, Kyoto University, Kyoto 606-8502, Japan; [b]Academic Assembly, Institute of Agriculture, Shinshu University, Nagano 399-4598, Japan; [c]Research Institute for Bioresources and Biotechnology, Ishikawa Prefectural University, Ishikawa 921-8836, Japan; [d]Graduate School of Technology, Industrial and Social Sciences, Tokushima University, Tokushima 770-8513, Japan; [e]Department of Molecular Microbiology, Tokyo University of Agriculture, Tokyo 156-8502, Japan; and [f]Iwate Biotechnology Research Center, Iwate 024-0003, Japan

Edited by Paul Schulze-Lefert, Max Planck Institute for Plant Breeding Research, Cologne, Germany, and approved November 21, 2018 (received for review April 27, 2018)

Plant pathogens have optimized their own effector sets to adapt to their hosts. However, certain effectors, regarded as core effectors, are conserved among various pathogens, and may therefore play an important and common role in pathogen virulence. We report here that the widely distributed fungal effector NIS1 targets host immune components that transmit signaling from pattern recognition receptors (PRRs) in plants. NIS1 from two *Colletotrichum* spp. suppressed the hypersensitive response and oxidative burst, both of which are induced by pathogen-derived molecules, in *Nicotiana benthamiana*. *Magnaporthe oryzae* NIS1 also suppressed the two defense responses, although this pathogen likely acquired the *NIS1* gene via horizontal transfer from Basidiomycota. Interestingly, the root endophyte *Colletotrichum tofieldiae* also possesses a *NIS1* homolog that can suppress the oxidative burst in *N. benthamiana*. We show that NIS1 of multiple pathogens commonly interacts with the PRR-associated kinases BAK1 and BIK1, thereby inhibiting their kinase activities and the BIK1-NADPH oxidase interaction. Furthermore, mutations in the NIS1-targeting proteins, i.e., BAK1 and BIK1, in *Arabidopsis thaliana* also resulted in reduced immunity to *Colletotrichum* fungi. Finally, *M. oryzae* lacking *NIS1* displayed significantly reduced virulence on rice and barley, its hosts. Our study therefore reveals that a broad range of filamentous fungi maintain and utilize the core effector NIS1 to establish infection in their host plants and perhaps also beneficial interactions, by targeting conserved and central PRR-associated kinases that are also known to be targeted by bacterial effectors.

BAK1 | BIK1 | core effector | PAMP-triggered immunity | phytopathogenic fungi

Plants have evolved two layers of antimicrobial defenses: pathogen-associated molecular pattern (PAMP)-triggered immunity (PTI) and effector-triggered immunity (ETI). PTI is mediated by membrane-embedded receptor-like proteins (RLPs), receptor-like kinases (RLKs) and receptor-like cytoplasmic kinases (RLCKs), whereas ETI generally occurs when cytoplasmic resistance (R) proteins detect specific pathogen effectors (1).

The immune kinases BAK1/SERK3 and BIK1 have been studied extensively in *Arabidopsis thaliana* as the central regulatory RLK and RLCK, respectively, working with multiple pattern recognition receptors for PAMP sensing and signaling (2–6). FLS2, another well-characterized RLK that recognizes the bacterial PAMP flagellin (flg22), recruits BAK1 upon ligand perception to initiate PTI signaling (2, 3, 7). In contrast, BIK1 forms a complex with FLS2 in the steady state (4, 5). Upon flg22 elicitation, BAK1 associates with FLS2 and phosphorylates BIK1; activated BIK1 then phosphorylates BAK1 and FLS2 before dissociating from the FLS2-BAK1 complex to transmit the signal to the downstream pathway (4, 5, 8). Phosphorylated BIK1 also activates the NADPH oxidase RBOHD through phosphorylation events to trigger a reactive oxygen species (ROS) burst, which is one of the earliest PTI responses (9, 10).

Many types of bacterial pathogen effectors target these RLK- and RLCK-type kinases. For example, *Pseudomonas syringae* AvrPto, AvrPtoB, HopF2, and HopB1 target BAK1, and *Xanthomonas oryzae* Xoo2875 targets OsBAK1 (the BAK1 homolog in rice) (11–14). AvrPto and AvrPtoB bind to BAK1 and interfere with formation of the FLS2-BAK1 complex (11). On the other hand, *P. syringae* AvrPphB and *Xanthomonas campestris* AvrAC target BIK1 (5, 15). AvrPphB, a cysteine protease, degrades PBS1-like kinases, including BIK1 (5), while the uridylyl transferase AvrAC conceals important phosphorylation sites in the activation loop of BIK1 (15). These findings strongly suggested that inhibiting these RLK- and RLCK-type kinases is advantageous to bacterial pathogens. However, it remained unclear whether this strategy is also employed by fungal and oomycete pathogens.

Our knowledge of the molecular functions of fungal and oomycete effectors is now expanding. The reported functions of these effectors are highly diverse and include inhibition of host-secreted lytic enzymes (16, 17), modulation of the plant ubiquitination system (18), autophagy (19), and blocking of the exposure of the fungal PAMP chitin to its corresponding receptor(s) in plants (20, 21).

Here we report that a so-called "core" effector named necrosis-inducing secreted protein 1 (NIS1), which is highly conserved in filamentous fungal plant pathogens, has the ability to target RLKs such as BAK1 and the RLCK BIK1 and thereby to impair PTI signaling. Core effectors can be defined by their

Significance

Multiple effectors of bacterial pathogens target immune kinases such as BAK1 and BIK1, but it is unclear whether this strategy is employed by fungal pathogens. We reveal here that a fungal effector named NIS1 is broadly conserved in filamentous fungi in the Ascomycota and Basidiomycota, thus being regarded as a core effector, and has the ability to suppress PAMP-triggered immunity. Importantly, NIS1 targets BAK1 and BIK1, interfering with their essential functions for immune activation upon pathogen recognition. Multifaceted analyses including the knockout of *NIS1* revealed that it plays a critical role in fungal infection. These findings demonstrate that to infect host plants, filamentous fungi deploy a core effector that attacks conserved immune kinases critical for the ancestral defense system.

Author contributions: Y.T. designed research; H.I., Y.I., M.M., K.Y., Y.O., H.S., A.U., S.K., A.K., and S.S.-O. performed research; H.I., Y.I., S.K., A.K., S.S.-O., and Y.T. analyzed data; and H.I., Y.I., M.M., H.S., R.T., and Y.T. wrote the paper.

The authors declare no conflict of interest.

This article is a PNAS Direct Submission.

[1]To whom correspondence should be addressed. Email: ytakano@kais.kyoto-u.ac.jp.

This article contains supporting information online at www.pnas.org/lookup/suppl/doi:10.1073/pnas.1807297116/-/DCSupplemental.

Published online December 24, 2018.

wide distribution among strains of a particular pathogen. For example, high-throughput genome sequencing of 65 strains of *Xanthomonas axonopodis* pv. *manihotis*, the causal agent of cassava bacterial blight, revealed that all strains shared nine common effectors, indicating that these nine are core effectors in this bacterial pathogen (22). On the other hand, extensive genome analyses on fungal pathogens also reveal the presence of abundant homologous effector proteins across different species, which are likewise widely defined as core effectors. NIS1 was first identified in cucumber anthracnose fungus, *Colletotrichum orbiculare*, as an effector that causes cell death in *Nicotiana benthamiana* (*Nb*) after *Agrobacterium*-mediated transient expression (23). Notably, this effector was found to be broadly conserved in filamentous fungal pathogens, and we therefore considered NIS1 as a putative core effector. However, deletion of *NIS1* had no effect on *C. orbiculare* virulence on its natural host, cucumber. Since *C. orbiculare* infects *Nb* in addition to Cucurbitaceae (24), we also inoculated the *nis1*Δ strain of *C. orbiculare* onto *Nb*; again, however, the mutant exhibited WT-like virulence on *Nb*. Therefore, the molecular and physiological function of this effector remained elusive.

In this study, we show that *C. orbiculare* NIS1, as well as NIS1 homologs of the crucifer anthracnose fungus *Colletotrichum higginsianum* and the rice blast fungus *Magnaporthe oryzae*, commonly suppress both hypersensitive response (HR) cell death triggered by the oomycete PAMP INF1 and ROS generation triggered by flg22 and the fungal PAMP chitin in *Nb*. These findings indicate that NIS1 suppresses multiple PTI responses in *Nb*. Our study demonstrates that NIS1 targets the RLK BAK1 and its orthologs in other plants, and also the RLCK BIK1, both of which are critical for PTI. The study also revealed that both BAK1 and BIK1 targeted by NIS1 are critical for plant immunity in *Arabidipsis* toward *Colletotrichum* fungi. We found that transient expression of NIS1 in *Nb* enhanced susceptibility to *C. orbiculare*. Furthermore, targeted gene disruption of *NIS1* in *M. oryzae* resulted in a severe reduction of virulence on both barley and rice susceptible cultivars, indicating the importance of the conserved effector NIS1 for fungal virulence.

Our data show that lineages of pathogens as different as bacteria and fungi share an effector-mediated strategy to interfere with immune kinases that transmit signaling from pathogen-recognizing receptors, suggesting that this effector innovation in phytopathogens has been essential to cope with PTI, which is probably universal in plants. The finding that NIS1 is conserved in a broad range of filamentous fungi in both Ascomycota and Basidiomycota also tells us that the effector NIS1 was already present in the common ancestor of these phyla and has been evolutionarily maintained to facilitate plant infection.

Results

The Conserved Filamentous Fungal Effector NIS1 Suppresses INF1-Induced Cell Death and Interacts with BAK1. We previously identified the effector NIS1 (hereafter called CoNIS1) from the hemibiotroph *C. orbiculare* as a secreted protein that induces cell death in *Nb* (23). We found 219 of putative CoNIS1 homologs in UniProtKB (*SI Appendix*, Table S1). CoNIS1 homologs are conserved in a broad range of fungi belonging to Sordariomycetes, Dothideomycetes, Eurotiomycetes, Orbiliomycetes, and Leotiomycetes in the Ascomycota, and to Exobasidiomycetes, Agaricomycetes, and Tremellomycetes in the Basidiomycota, which include numerous pathogenic fungi (Fig. 1 and *SI Appendix*, Fig. S1). This suggests that NIS1 is an evolutionarily ancient effector, and its broad conservation implies the importance of NIS1 as a possible core effector in fungal pathogens. Intriguingly, we also found that the root endophyte *C. tofieldiae* possesses a NIS1 homolog (Fig. 1 and *SI Appendix*, Fig. S1), indicating that the conservation of NIS1 is not limited to pathogens but extends to beneficial species (25).

We next investigated whether CoNIS1 can suppress plant immune responses. The well-known oomycete PAMP elicitor INF1 strongly induces cell death in a restricted number of *Nicotiana* and *Solanum* species within solanaceous plants, including *Nb* (26, 27). Because *C. orbiculare* infects *Nb* (24), and because INF1-induced cell death is reportedly suppressed not only by oomycete effectors but also by effectors of organisms in different kingdoms (28, 29), we first examined possible effects of CoNIS1 on the INF1-elicited immune response in *Nb*. Transient expression of INF1 by agroinfiltration induces rapid HR cell

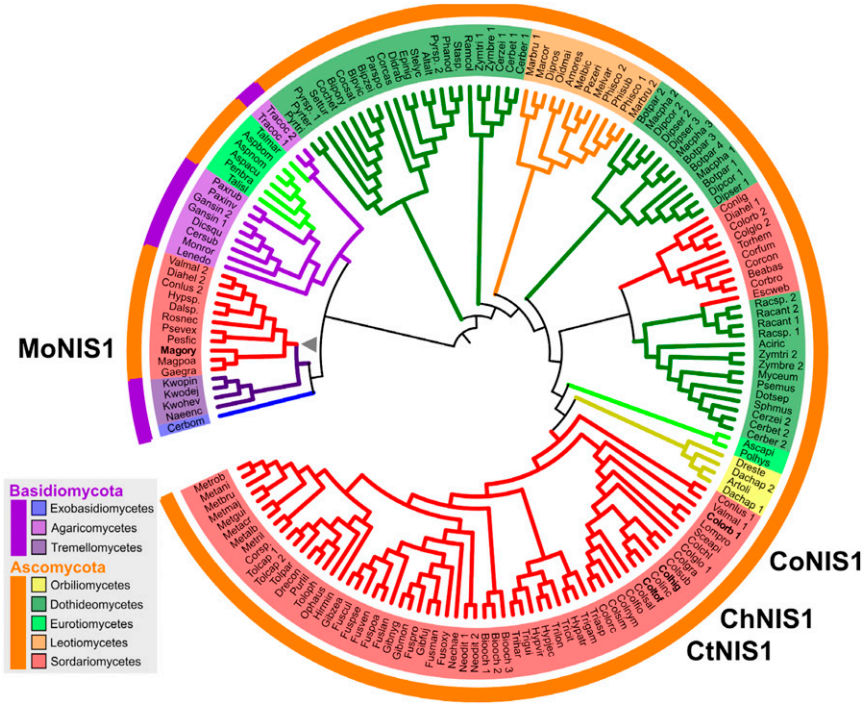

Fig. 1. *NIS1* is widely distributed among fungal lineages of Ascomycota and Basidiomycota. An unscaled phylogenetic tree of selected NIS1 homologs reconstructed by treefixDTL (62) is shown. Out of 219 putative NIS1 homologs, we selected 171 homologs by removing redundant information using the following selection criteria: (*i*) When multiple homologs with identical sequences were present, one homolog was arbitrarily chosen and retained; and (*ii*) when multiple homologs from a different strain of the same species were present, homologs from an arbitrarily chosen strain was retained. Leaf labels represent abbreviated names of the species to which the NIS1 homologs belong. When multiple NIS1 homologs are present in a species, unique numbers were assigned to each leaf label. Leaf labels and nodes are color coded according to class. The track outside the tree represents fungal phylum. NIS1 homologs from *C. orbiculare* (CoNIS1), *C. higginsianum* (ChNIS1), *C. tofieldiae* (CtNIS1), and *Magnaporthe oryzae* (MoNIS1) are shown in bold. Potential transfer from Basidiomycota (Tremellomycetes) to Ascomycota (Sordariomycetes) is indicated by the gray arrowhead. For full species and gene names, see *SI Appendix*, Tables S1 and S2.

death in *Nb* within 2 d postinoculation (dpi) (30); this is much faster than CoNIS1-induced cell death, which is first observed after 5 dpi. Taking advantage of the different timing between CoNIS1- and INF1-induced necrosis, we tested whether CoNIS1 can suppress INF1-induced cell death. We found that INF1-induced cell death was clearly suppressed at 3 dpi of *Agrobacterium* harboring a plasmid expressing INF1 by pre-expression of CoNIS1 (Fig. 2*A* and *SI Appendix*, Fig. S2). CoNIS1 eventually caused cell death at 6 dpi (*SI Appendix*, Fig. S3). Moreover, the NIS1 homolog of crucifer anthracnose fungus *C. higginsianum* (ChNIS1) also suppressed INF1-induced cell death (Fig. 2*A* and *SI Appendix*, Fig. S2). We previously found that the NIS1 homolog of the rice blast fungus *M. oryzae* (MoNIS1) did not induce necrotic lesions in *Nb* (23), in contrast to CoNIS1 and ChNIS1, indicating that MoNIS1 is functionally distinct from the *Colletotrichum* NIS1s. Interestingly, the phylogenetic analysis revealed that MoNIS1 is distantly related to CoNIS1 and ChNIS1 but more closely related to NIS1 homologs in the Basidiomycota (Fig. 1). Comparisons of NIS1 phylogeny and species phylogeny suggest that the common ancestor of Magnaporthales, Diaporthales, and Xylariales gained a *NIS1* gene from Tremellomycetes (*SI Appendix*, Fig. S4).

Remarkably, MoNIS1 also suppressed INF1-induced cell death (Fig. 2*A* and *SI Appendix*, Fig. S2), despite its evolutionary remoteness from NIS1 homologs of other Ascomycete fungi (Fig. 1 and *SI Appendix*, Fig. S4). Therefore, the fungal effector NIS1, widely conserved in fungal pathogens, commonly suppresses INF1-induced PTI in *Nb*. It is noteworthy that MoNIS1 failed to induce necrotic lesions in *Nb* (23), thus uncoupling the suppression of INF1-induced cell death from the activity of NIS1 itself to induce cell death in *Nb*.

BAK1, a member of the SERK family, is a central regulator required for recognition of multiple PAMPs in *Nb* and *Arabidopsis* (2, 3, 6). Importantly, silencing of the *BAK1* homolog of *Nb*, *NbSerk3*, canceled INF1-induced cell death in *Nb* (3, 31). It was also reported that a receptor for INF1, named ELR, identified in the wild potato *Solanum microdontum*, associates with BAK1 homologs of potato (32), further supporting the role of the BAK1 homolog in INF1-induced cell death in *Nb*.

Therefore, to assess the possibility that NIS1 targets BAK1, we looked for an interaction of BAK1 with CoNIS1 and MoNIS1 in a coimmunoprecipitation (co-IP) analysis in *Nb*. Green fluorescent protein (GFP)-tagged BAK1 was expressed together with each NIS1 homolog in *Nb*, and subsequent co-IP analysis using anti-GFP beads revealed that both CoNIS1 and MoNIS1 coimmunoprecipitated with BAK1-GFP (Fig. 2*B*), indicating their interaction with BAK1 in planta. CoNIS1 also associated with NbSERK3 (Fig. 2*B*). A yeast two-hybrid assay revealed that both CoNIS1 and MoNIS1 lacking the signal peptide (SP) interact with the cytoplasmic region of BAK1 (Fig. 2*C*). We then transiently expressed a functional mCherry-fused MoNIS1 and BAK1-GFP in *Nb* (*SI Appendix*, Fig. S5). Part of the mCherry signal was detected in the cytosol, and the remainder colocalized with the signal of BAK1-GFP located in the cell's plasma membrane in *Nb* (Fig. 2*D*). The result is consistent with our previous report that mCherry-fused CoNIS1 secreted by *M. oryzae* translocated into rice cells (33), as well as accumulating in a biotrophic interfacial complex (BIC) (34, 35). Collectively, these findings suggest that NIS1 acts as a cytoplasmic effector and has the ability to interact with the cytoplasmic region of BAK1. CoNIS1 and MoNIS1 also interacted with BKK1 (*SI Appendix*, Fig. S6), a close paralog of BAK1 in *Arabidopsis* that can form complexes with PAMP receptors on ligand binding and transmit PTI signals (6).

To gain further insights into the NIS1-BAK1 interaction, we performed a deletion analysis of CoNIS1 (Fig. 3*A*). We found that CoNIS1 lacking the C-terminal 30 amino acids (CoNIS1ΔC30) suppressed INF1-induced cell death (Fig. 3*A* and *SI Appendix*, Fig. S2) and still interacted with BAK1 (Fig. 3*B*). In contrast, CoNIS1 lacking the C-terminal 60 amino acids (CoNIS1ΔC60) failed to suppress INF1-induced cell death and displayed a severe reduction in BAK1 association (Fig. 3 *A* and *B* and *SI Appendix*, Fig. S2). These findings illustrate a correlation between suppression of INF1-induced cell death and interaction with BAK1.

The clear difference between CoNIS1ΔC30 and CoNIS1ΔC60 in the suppression assay for INF1-induced cell death implied that the C-terminal 31- to 60-amino acid region is important for the cell death suppression. To assess this, we performed alanine-scanning

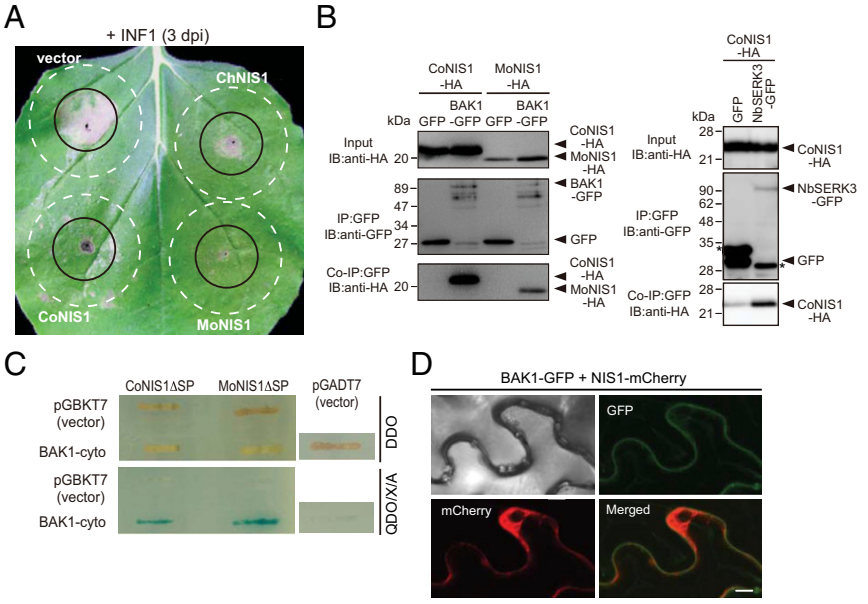

Fig. 2. NIS1 suppresses INF1-induced cell death and directly interacts with BAK1. (*A*) Suppression of INF1-induced cell death by the NIS1 homologs of *C. orbiculare*, *C. higginsianum*, and *M. oryzae*. Infiltration sites of *A. tumefaciens* harboring a plasmid expressing each NIS1 homolog or *A. tumefaciens* harboring the empty plasmid pBICP35 as a vector control (vector) (dashed white circles) were challenged with *A. tumefaciens* harboring a plasmid expressing INF1 (solid black circles) in *Nb*. The photograph was taken at 3 dpi. Similar results were obtained in two additional experiments. (*B*) Co-IP of BAK1 and NbSERK3 with NIS1 homologs. BAK1-GFP, NbSERK3-GFP, or GFP (control) was transiently coexpressed with CoNIS1-HA or MoNIS1-HA in *Nb*. Total protein extracts were subjected to IP with anti-GFP magnetic beads followed by immunoblotting (IB) with anti-HA and anti-GFP antibodies. Asterisks indicate truncated or modified forms of the expressed proteins that were detected by anti-GFP antibody. Similar results were obtained in two additional experiments. (*C*) Interaction of NIS1 homologs lacking a signal peptide with the cytoplasmic region of *Arabidopsis* BAK1 (BAK1-cyto) in yeast two-hybrid assays. The interactions were examined by assessing growth on the selective medium QDO/X/A (SD/–Ade/–His/–Leu/–Trp/x-a-Gal/Aba). DDO (SD/–Leu/–Trp) medium was used for a mating control. Similar results were obtained from one additional experiment. (*D*) A part of MoNIS1-mCherry signal was colocalized with BAK1-GFP1 located in the plasma membrane in *Nb*. BAK1-GFP1 and a functional MoNIS1-mCherry were transiently expressed in *Nb* via agroinfiltration. At 2 dpi, the fluorescence signal was examined under a confocal microspope. (Scale bar = 10 μm.)

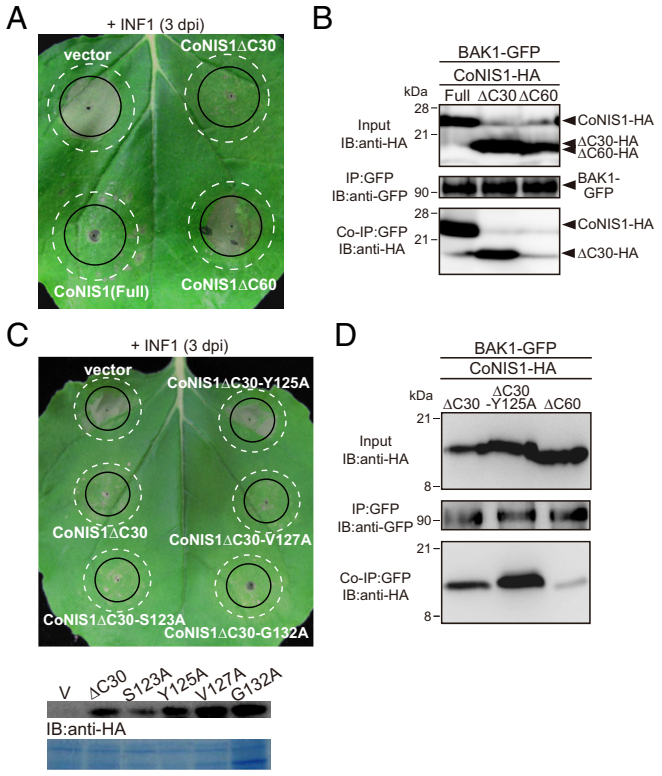

Fig. 3. The ability of NIS1 to suppress INF1-induced cell death correlates with NIS1-BAK1 interaction. (*A*) Suppression assay of INF1-induced cell death by C-terminal truncation mutants of CoNIS1. Infiltration sites of *A. tumefaciens* harboring a plasmid expressing CoNIS1-HA, CoNIS1ΔC30-HA, or CoNIS1ΔC60-HA, or *A. tumefaciens* harboring the empty plasmid pBICP35 as a vector control (vector) (dashed white circles), were challenged with *A. tumefaciens* harboring a plasmid expressing INF1 (solid black circles) in *Nb*. The photograph was taken at 3 dpi. Similar results were obtained in two additional experiments. (*B*) Co-IP of *Arabidopsis* BAK1 and the HA-tagged C-terminal truncation series of CoNIS1. BAK1-GFP was transiently coexpressed with CoNIS1-HA, CoNIS1ΔC30-HA, or CoNIS1ΔC60-HA in *Nb*. Total protein extracts were subjected to IP with anti-GFP magnetic beads followed by IB with anti-HA and anti-GFP antibodies. Similar results were obtained in four additional experiments. (*C*) Suppression assay of INF1-induced cell death by CoNIS1ΔC30 with an Ala point mutation series. Infiltration sites of *A. tumefaciens* harboring a plasmid expressing CoNIS1ΔC30-HA, CoNIS1ΔC30-S123A-HA, CoNIS1ΔC30-Y125A-HA, CoNIS1ΔC30-V127A-HA, or CoNIS1ΔC30-G132A-HA, or *A. tumefaciens* harboring the empty plasmid pBICP35 as a vector control (vector) (dashed white circles), were challenged with *A. tumefaciens* harboring a plasmid expressing INF1 (solid black circles) in *Nb*. The photograph was taken at 3 dpi. Protein extracts were analyzed by IB with anti-HA antibody (*Upper*). CBB staining was used as a loading control (*Lower*). Similar results were obtained in one additional experiment. (*D*) Y125 is dispensable for the interaction of CoNIS1ΔC30 with *Arabidopsis* BAK1. BAK1-GFP was transiently coexpressed with CoNIS1ΔC30-HA, CoNIS1ΔC30-Y125A-HA, or CoNIS1ΔC60-HA in *Nb*. Total protein extracts were subjected to IP with anti-GFP magnetic beads followed by IB with anti-HA and anti-GFP antibodies. Similar results were obtained from additional two independent experiments.

mutational analyses instead of further deletion. We selected amino acids located at the end of NIS1ΔC30 while considering the properties and conservation of each residue: Ser at position 123 to Ala (S123A), Tyr at 125 to Ala (Y125A), Val at 127 to Ala (V127A), and Gly at 132 to Ala (G132A) (*SI Appendix*, Fig. S1). The suppression assay for each of these mutants revealed that introducing the Y125A mutation abolished the ability of CoNIS1ΔC30 to suppress INF1-induced cell death although it had no effect on the protein's stability (Fig. 3*C*). Interestingly, CoNIS1ΔC30 carrying Y125A still interacted with BAK1 (Fig. 3*D*), implying that Y125A specifically reduces the interaction with NbSERK3 and its paralogs but not *Arabidopsis* BAK1. Alternatively, NIS1 might target unidentified components critical for INF1-induced cell death in addition to BAK1-type immune kinases. We also revealed that full-length CoNIS1 carrying Y125A still caused cell death in *Nb* (*SI Appendix*, Fig. S7), further supporting the uncoupling of the cell death-inducing activity from the ability to suppress INF1-induced cell death. Tyr-125 is moderately conserved in NIS1s of other fungal pathogens (41%) and its substituents are usually other aromatic amino acids, Phe (38%, including MoNIS1) or Trp (6%) (*SI Appendix*, Fig. S1).

NIS1 Inhibits PAMP-Induced ROS Generation and Binds to the RLCK BIK1. We investigated whether NIS1 can cancel different types of cell death in *Nb*. Transient expression of Avr3a, an avirulence protein of *Phytophthora infestans*, together with its cognate R protein R3a triggers HR cell death in *Nb* (30). Interestingly, MoNIS1 suppressed R3a/Avr3a-dependent HR cell death (*SI Appendix*, Fig. S8). We could not test this ability for CoNIS1 because of its own capacity to induce cell death in *Nb*. R3a/Avr3a-dependent HR cell death is not canceled in *NbSerk3*-silenced plants (36), implying that at least MoNIS1 has other targets in addition to BAK1. To assess whether NIS1 inhibits PTI responses that do not accompany an HR response, we measured ROS produced after flg22 treatment in *Nb* transiently expressing CoNIS1 or each NIS1 homolog (Fig. 4*A*). CoNIS1, ChNIS1, and MoNIS1 all blocked the ROS burst, demonstrating that this effector from multiple pathogens suppresses flg22-triggered ROS generation in *Nb*. CoNIS1ΔC30, but not CoNIS1ΔC60, also blocked the ROS burst (Fig. 4*A*). We further found that CoNIS1 and MoNIS1 suppressed ROS generation triggered by the fungal PAMP chitin in *Nb*, although the suppression activity of MoNIS1 was weaker than that of CoNIS1 (Fig. 4*B*). The finding that NIS1 can suppress more than one PAMP-induced ROS production pathway is consistent with the wide conservation of this effector among fungal pathogens.

BIK1 plays a critical role in ROS generation triggered by multiple PAMPs (flg22, elf18, and chitin) in *Arabidopsis* by directly interacting with and phosphorylating the NADPH oxidase RBOHD (9, 10). As shown above, NIS1 interacts with the cytoplasmic domain of BAK1/SERK3 and BKK1 (Fig. 2*C* and *SI Appendix*, Fig. S6), which is composed almost entirely of a serine/threonine protein kinase domain. The kinase domain of BIK1 shares 43% identity and 80% similarity with the cytoplasmic kinase domain of BAK1. Thus, we checked the potential interaction between NIS1 and BIK1 by co-IP assay in *Nb*. This revealed that CoNIS1 can indeed interact with BIK1 (Fig. 4*C*). Analysis of the truncated forms of CoNIS1 indicated that CoNIS1ΔC30, but not CoNIS1ΔC60, associates with BIK1 (Fig. 4*C*), suggesting that the binding modes of CoNIS1 to BIK1 and BAK1/SERK3 (Fig. 3*B*) are similar. MoNIS1 also interacts with BIK1 (Fig. 4*D*). These results indicate that NIS1 is able to associate with a RLCK, BIK1, as well as with RLKs including BAK1/SERK3.

As noted above, the phosphorylation of RBOHD by BIK1 results in a PAMP-dependent ROS burst (9, 10). Given that *Arabidopsis* BIK1 and RBOHD interact with each other in *Nb* (10), we asked whether CoNIS1 binding to BIK1 affects the BIK1-RBOHD interaction in *Nb*. Consistent with a previous report (10), we detected a BIK1-RBOHD interaction by co-IP assay using GFP-tagged BIK1 (Fig. 4*E*). Importantly, RBOHD protein coimmunoprecipitation with BIK1 almost completely disappeared in the presence of full-length CoNIS1 (Fig. 4*E*). On the other hand, the CoNIS1ΔC60 mutant, which lacks the ability to bind to BIK1, did not affect the amount of coimmunoprecipitating RBOHD. These results suggest that NIS1 blocks the interaction between BIK1 and RBOHD by targeting BIK1. The Y125A mutation abolished the ability of CoNIS1ΔC30 to suppress INF1-induced cell death. We then asked whether CoNIS1ΔC30-Y125A suppresses

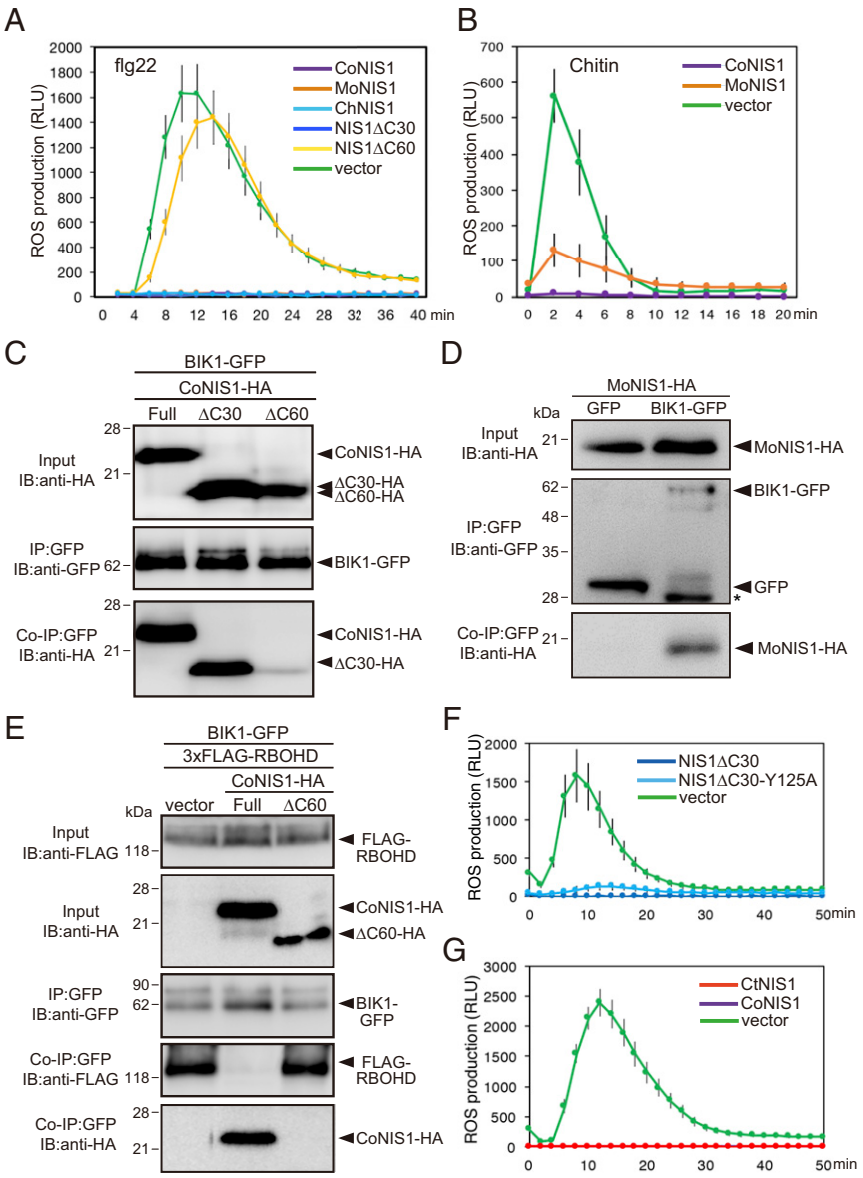

Fig. 4. NIS1 prevents BIK1-RBOHD interaction by targeting BIK1 and inhibits PAMP-triggered ROS generation. (*A*) Suppression of flg22-triggered ROS production by NIS1 in *Nb*. Total ROS production [represented as relative luminescence units (RLU)] by *Nb* transiently expressing CoNIS1-HA, MoNIS1-HA, ChNIS1-HA, CoNIS1ΔC30-HA, or CoNIS1ΔC60-HA, or harboring empty vector as control, was measured after treatment with 500 nM flg22. Results are average + SE ($n = 12$). Similar results were obtained in two additional experiments. (*B*) Suppression of chitin-triggered ROS production by NIS1 in *Nb*. Total ROS production (represented as RLU) by *Nb* transiently expressing CoNIS1-HA or MoNIS1-HA after treatment with 1 mg/mL chitin. Results are average + SE ($n = 12$). Similar results were obtained in two additional experiments. (*C*) Co-IP of *Arabidopsis* BIK1 with CoNIS1. BIK1-GFP or GFP (control) was transiently coexpressed with CoNIS1-HA, CoNIS1ΔC30-HA, or CoNIS1ΔC60-HA in *Nb*. Total protein extracts were subjected to IP with anti-GFP magnetic beads followed by IB with anti-HA and anti-GFP antibodies. Similar results were obtained in three additional experiments. (*D*) Co-IP of *Arabidopsis* BIK1 with MoNIS1. The asterisk marks a truncated form of the expressed protein that was detected by anti-GFP antibody. Similar results were obtained in three additional experiments. (*E*) Prevention of BIK1-RBOHD association by NIS1. Co-IP was performed in *Nb* transiently expressing BIK1-GFP and 3xFLAG-RBOHD with CoNIS1-HA or CoNIS1ΔC60-HA. *A. tumefaciens* harboring the empty plasmid pBICP35 was infiltrated (vector) as a control for the expression of CoNIS1-HA and CoNIS1ΔC60-HA. Total protein extracts were subjected to IP with anti-GFP magnetic beads followed by IB with anti-FLAG, anti-HA, and anti-GFP antibodies. Similar results were obtained from one additional experiment. (*F*) CoNIS1ΔC30-Y125A suppressed flg22-triggered ROS production in *Nb*. Similar results were obtained in one additional experiment. (*G*) NIS1 of the root endophyte *C. tofieldiae* suppressed flg22-triggered ROS production in *Nb*. Similar results were obtained in two additional experiment.

flg22-triggered ROS generation in *Nb*. Notably, CoNIS1ΔC30-Y125A clearly suppressed ROS generation (Fig. 4*F*), which is likely consistent with the finding that CoNIS1ΔC30-Y125A maintains the ability to interact with one of its targets, namely BAK1 (Fig. 3*D*).

As mentioned above, we found that a NIS1 homolog is conserved in a root endophyte, *C. tofieldiae* (Fig. 1 and *SI Appendix*, Fig. S1) (25). Interestingly, we noticed that *C. tofieldiae* expresses the *NIS1* homolog abundantly during *Arabidopsis* colonization at 6, 10, 16, and 24 dpi by referring to deposited RNA sequencing data of Hiruma et al. (25). This raises the possibility that *C. tofieldiae* utilizes NIS1 for its beneficial interaction with *Arabidopsis*. Therefore, we asked whether the *C. tofieldiae* NIS1 homolog is able to suppress plant immune responses in the same way as the NIS1s of the pathogens by performing the suppression assay for flg22-triggered ROS generation in *Nb*. Remarkably, *C. tofieldiae* NIS1 also suppressed flg22-triggered ROS generation (Fig. 4*G*).

NIS1 Inhibits the Kinase Activity of Both BAK1 and BIK1. We found that NIS1 has no detectable effect on the stability of BAK1 or BIK1 in planta, suggesting that the fungal effector NIS1 possesses no activity to degrade or cleave these RLK and RLCK members (Fig. 5*A*). In PTI, phosphorylation relaying by RLKs (FLS2, BAK1, etc.) and RLCKs (BIK1, etc.) is critical for the initiation of downstream signaling (37). To investigate whether NIS1 affects the kinase activities of BAK1 and/or BIK1, we performed an in vitro kinase assay with these proteins, purified using a maltose binding protein (MBP) tag, in the presence or absence of CoNIS1 protein. We prepared a semipurified fraction containing CoNIS1 lacking the SP secreted from tobacco BY2 cells expressing this NIS1. For BAK1, we prepared the cytoplasmic domain (CD) of BAK1 instead of the full-length version. The assay revealed that CoNIS1 strongly inhibited autophosphorylation of MBP-BAK1CD (Fig. 5*B*). We also found that CoNIS1 inhibited autophosphorylation of MBP-BIK1 (Fig. 5*C*). These results suggest that NIS1 binds to BAK1 and BIK1 and then inhibits their kinase activity.

***Arabidopsis* BAK1 and BIK1 Targeted by NIS1 Are Critical for Immunity to *Colletotrichum* Fungi.** Because NIS1 binds to RLKs (BAK1/SERK3 and BKK1) and a RLCK (BIK1) and inhibits their kinase activity, we then investigated the impact of the loss of these RLK/RLCKs on *Arabidopsis* immunity to *Colletotrichum* fungi. We first inoculated the adapted *C. higginsianum* onto the *Arabidopsis bak1-5* mutant. The *bak1-5* mutation is a semidominant allele of BAK1 with a specific phenotype related to PAMP responsiveness (38). Quantitative assay for the size of developed lesions revealed that *C. higginsianum* displayed enhanced virulence to the *bak1-5* mutant (Fig. 6*A*). We then inoculated *C. higginsianum* onto the *bik1* mutant and the *bik1 pbl1* mutant because PBL1 is highly similar to, and displays partial functional redundancy with BIK1 (5). *C. higginsianum* also showed enhanced virulence to *bik1* and *bik1 pbl1*, similar to *bak1-5* (Fig. 6*A*). Microscopic analysis revealed that the appressorium-mediated entry rate in *bak1-5* was higher than in the wild-type (WT) plant (Fig. 6*B*). We also inoculated nonadapted *Colletotrichum tropicale* present in the *Colletotrichum gloeosporioides* complex (previously reported as *C. gloeosporioides*) onto these mutants together with a mutant defective in *PEN2* (*PENETRATION 2*), which is critical for nonhost resistance against *C. tropicale* (39, 40). We found that the nonadapted *C. tropicale* developed clear lesions in the *pen2*, *bak1-5*, *bik1*, and *bik1 pbl1* mutants but not in the wild-type plant (Fig. 6*C*). *C. tropicale* entry rates also increased in both *bak1-5* and *bik1 pbl1* compared with the wild-type plant (Fig. 6*D*). Collectively, these results suggest that the RLK and RLCK targeted by NIS1 play an important role in *Arabidopsis* immunity toward both adapted and nonadapted *Colletotrichum* fungi, including preinvasive resistance that is critical for pathogen entry control.

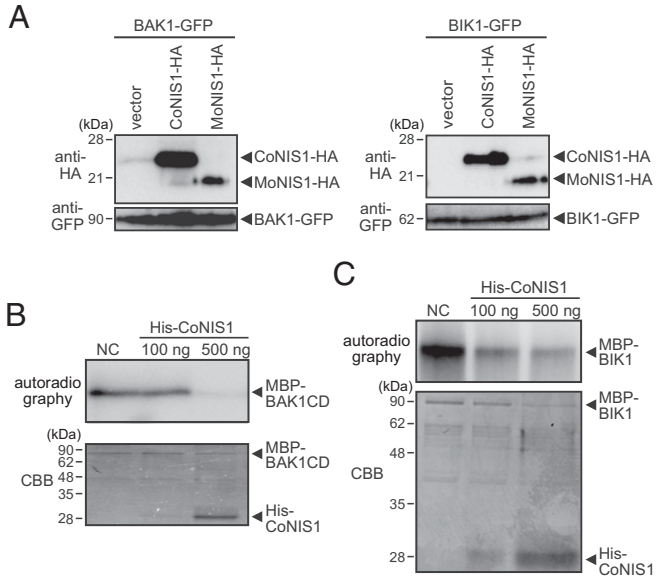

Fig. 5. NIS1 inhibits the kinase activity of both BAK1 and BIK1. (*A*) Effects of NIS1 homologs (CoNIS1 and MoNIS1) on protein stability of BAK1 (*Left*) and BIK1 (*Right*). CoNIS1-HA or MoNIS1-HA were transiently coexpressed with BAK1-GFP or BIK1-GFP in *Nb*. *A. tumefaciens* harboring the empty plasmid pBICP35 was infiltrated (vector) as a control for the expression of CoNIS1-HA and MoNIS1-HA. Protein extracts were analyzed by immunoblotting with anti-HA and anti-GFP antibodies. (*B*) NIS1 inhibits autophosphorylation of BAK1. Purified MBP-fused BAK1 cytoplasmic domain (MBP-BAK1CD) were incubated with His-tagged CoNIS1 proteins purified from the culture medium of BY-2 cells secreting CoNIS1 (CoNIS1, 500 ng). We incubated MBP-fused kinase proteins with the equivalent fraction purified from the culture medium of BY-2 cells that do not secrete CoNIS1 as a negative control (NC). The His-tagged CoNIS1 protein fraction was also diluted fivefold with kinase reaction buffer and used for the assay (CoNIS1, 100 ng). In vitro kinase assay using [γ-^{32}P] ATP was performed and autophosphorylation was visualized by autoradiography. CBB was used as a loading control. Similar results were obtained from one additional experiment. (*C*) NIS1 inhibits autophosphorylation of BIK1. Purified MBP-fused BIK1 (MBP-BIK1) were subjected to the analysis described in B. Similar results were obtained from three additional experiments.

NIS1 Contributes to Fungal Virulence. We previously reported that targeted deletion of *CoNIS1* did not affect the virulence of *C. orbiculare* on *Nb* or cucumber, its natural host (23). This suggested either a functional redundancy of another effector(s) with CoNIS1 in *C. orbiculare*, or that CoNIS1 does not contribute to the virulence of *C. orbiculare*. To clarify this, we tested whether *Nb* expressing *NIS1* displays enhanced susceptibility to *C. orbiculare*. We transiently expressed MoNIS1 in *Nb* leaves under the control of the cauliflower mosaic virus 35S promoter and then inoculated *C. orbiculare* onto the treated leaves. We expressed MoNIS1 instead of CoNIS1 because CoNIS1, but not MoNIS1, induced necrotic lesions, which would interfere with the evaluation of lesion development by the pathogen. The result revealed that MoNIS1 expression significantly enhanced lesion development by *C. orbiculare* (Fig. 7 *A* and *B*). This finding suggests that the conserved effector NIS1 has a role in the virulence of *C. orbiculare* against plants including *Nb*.

We also generated a *MoNIS1* knockout (*monis1*Δ) mutant of *M. oryzae* by targeted gene disruption. The *monis1*Δ mutant exhibited normal colony growth, the same as the WT strain (*SI Appendix*, Fig. S9 *A* and *B*). Remarkably, inoculation assays of the mutant on barley and rice revealed that it possessed severely reduced virulence on both hosts compared with WT (Fig. 7 *C* and *D*); this phenotype was complemented by reintroduction of *MoNIS1* (*SI Appendix*, Fig. S9*C*). The effector MoNIS1 therefore plays a critical role in host infection by *M. oryzae*. Strikingly, the virulence of the *monis1*Δ mutant was restored by introducing a genomic region encompassing *CoNIS1* (Fig. 7*C*). It has been reported that *OsBAK1* is involved in rice immunity against *M. oryzae* (41), and we found that both CoNIS1 and MoNIS1 indeed interact with OsBAK1 transiently expressed in *Nb* (Fig. 7*E*).

Discussion

The work presented here has revealed that the fungal core effector NIS1 targets BAK1/SERK3 and BIK1, key kinases in plant PTI signaling that have only previously been reported to be targeted by bacterial effectors (5, 11, 13, 15). It was previously reported that the fungal effector Pep1 is essential for host penetration by *Ustilago maydis* (42). Pep1 is conserved in Ustilaginaceae, where it is regarded as a core effector (43), but not

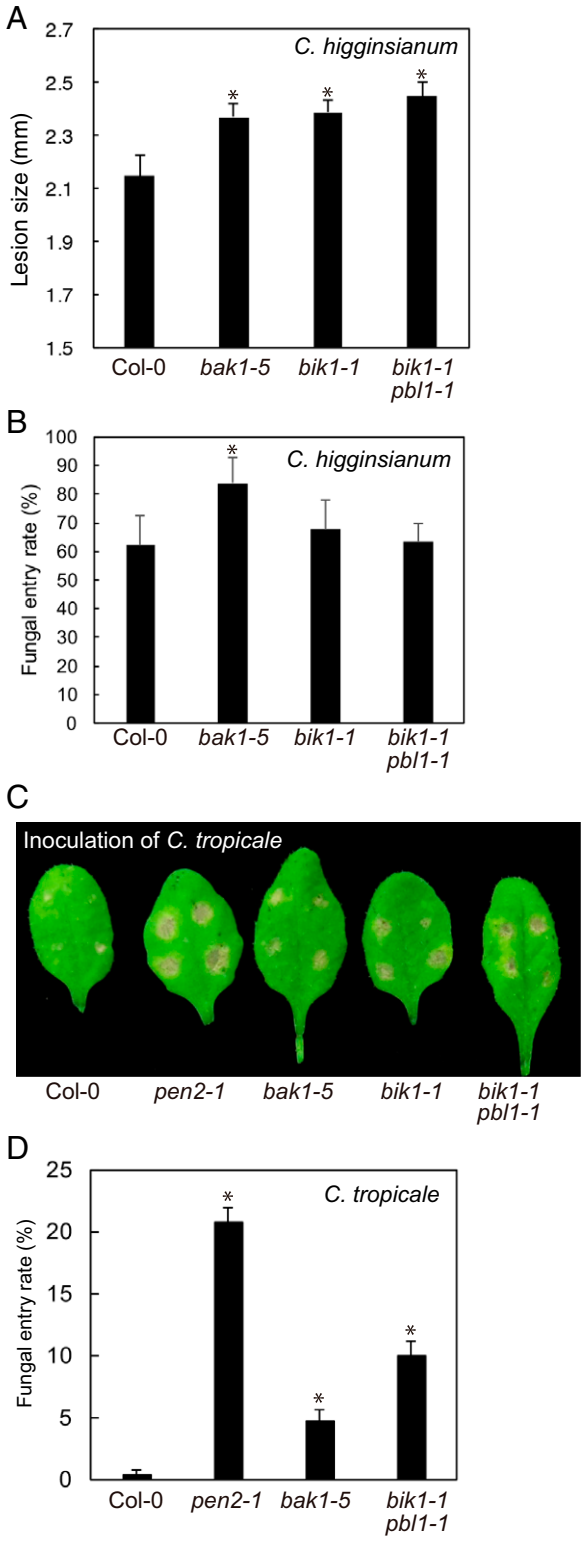

Fig. 6. BAK1 and BIK1 targeted by NIS1 are involved in *Arabidopsis* immunity toward *Colletotrichum* fungi. (*A*) Quantification of lesion size of adapted *C. higginsianum* on *Arabidopsis* mutants. A conidial suspension of *C. higginsianum* (2.5×10^5 conidia per milliliter) was inoculated onto leaves of *Arabidopsis* WT (Col-0), *bak1-5*, *bik1-1*, and *bik1-1 pbl1-1*. Lesion sizes were determined 5 dpi. At least 50 lesions in each experiment were measured. Means and SD were calculated from three independent experiments. The statistical significance of differences between means was determined by two-tailed *t* test. $*P < 0.05$ (comparison with Col-0). (*B*) Quantitative analysis of *C. higginsianum* entry. Conidia of *C. higginsianum* (5×10^5 conidia per milliliter) were inoculated onto each plant line, as above, and inoculated plants were incubated for 3 d. One hundred appressoria produced by *C. higginsianum* on each plant were observed. Means and SD were calculated from five independent plant samples. The statistical significance of differences between means was determined by two-tailed *t* test. $*P < 0.01$ (comparison with Col-0). (*C*) Inoculation assay of nonadapted *C. tropicale* on *Arabidopsis* mutants. A conidial suspension of *C. tropicale* with 0.1% glucose (5×10^5 conidia per milliliter) was inoculated onto *Arabidopsis* WT (Col-0), *pen2-1*, *bak1-5*, *bik1-1*, and *bik1-1 pbl1-1*. Inoculated plants were incubated for 4 d. (*D*) Quantitative analysis of *C. tropicale* entry. Conidia of *C. tropicale* with 0.05% glucose were inoculated onto each plant line, as above, and inoculated plants were incubated for 14 h. At least 100 conidia were observed in each experiment. Means and SD were calculated from three independent experiments. The statistical significance of differences between means was determined by two-tailed *t* test. $*P < 0.01$ (comparison with Col-0).

outside this family. In contrast, the effector NIS1 is conserved in fungi belonging to both Ascomycota and Basidiomycota. Thus, we consider that NIS1 is a core effector, acquired anciently by fungal pathogens. This idea is supported by our finding that NIS1 targets PAMP recognition and signaling machineries that are probably universally conserved in higher plants. Indeed, it was recently reported that the moss *Physcomitrella patens* recognizes chitin and mounts defense responses via the RLK CERK1 (44), indicating that RLK-dependent PAMP recognition is an ancestral system in plants.

Since the sequence of NIS1 has no similarity to bacterial effectors that target RLKs and RLCKs, our findings also suggest independent effector innovation in bacterial and fungal pathogens to attack RLK and RLCK class kinases that are critical for PTI. Independent effector innovation at the interkingdom level has also been detected in multiple plant proteins such as Rcr3 protease, which is targeted by protease inhibitors from pathogenic fungi, oomycetes, and nematodes (17, 45, 46). BAK1-related RLKs and BIK1-related RLCKs are well conserved and critical for PTI; thus, we consider that once a fungus had innovated NIS1, it was essential to maintain it as a core effector during evolution. In contrast to NIS1, bacterial effectors that attack RLKs and RLCKs, such as AvrPto, are not broadly conserved among bacterial pathogens. It remains unclear why this type of effector is not widely conserved among bacterial pathogens. As noted above, genome sequencing of 65 strains of *X. axonopodis* pv. *manihotis* identified nine core effectors that are shared by all tested strains of this bacterial pathogen (22). However, these effectors are not strongly conserved in *X. campestris*. Furthermore, there is no overlap between *X. campestris* and *P. syringae* core effectomes (47). In contrast, many putative core effectors are conserved in fungal species: for example, ~200 core effector-like genes are conserved in four different *Colletotrichum* species (48), suggesting that infection strategies based on core effectors, including NIS1, are more important in fungal pathogens than in bacterial pathogens.

The expression of CoNIS1 and ChNIS1, but not MoNIS1, caused necrotic lesion formation in *Nb* (23), whereas CoNIS1, ChNIS1, and MoNIS1 commonly suppressed INF1-induced cell death and PAMP-triggered ROS generation in *Nb* (Figs. 2*A* and 4*A*). CoNIS1 lacking its C-terminal 30 amino acids (CoNIS1ΔC30) strongly reduced necrotic lesion development (23) in comparison with full-length CoNIS1, and this region is missing in MoNIS1 (*SI Appendix*, Fig. S1). Thus, the corresponding region is dispensable for plant immune suppression but is important to induce necrotic lesions, possibly via plant recognition and activation of cell death as a counterdefense. In this context, it is notable that *C. orbiculare* deploys an effector, DN3, that can reduce CoNIS1-triggered plant cell death (23). *MoNIS1* is phylogenetically distant from *CoNIS1* and is likely to originate from an *NIS1* homolog of the Basidiomycota. Considering that *Valsa*

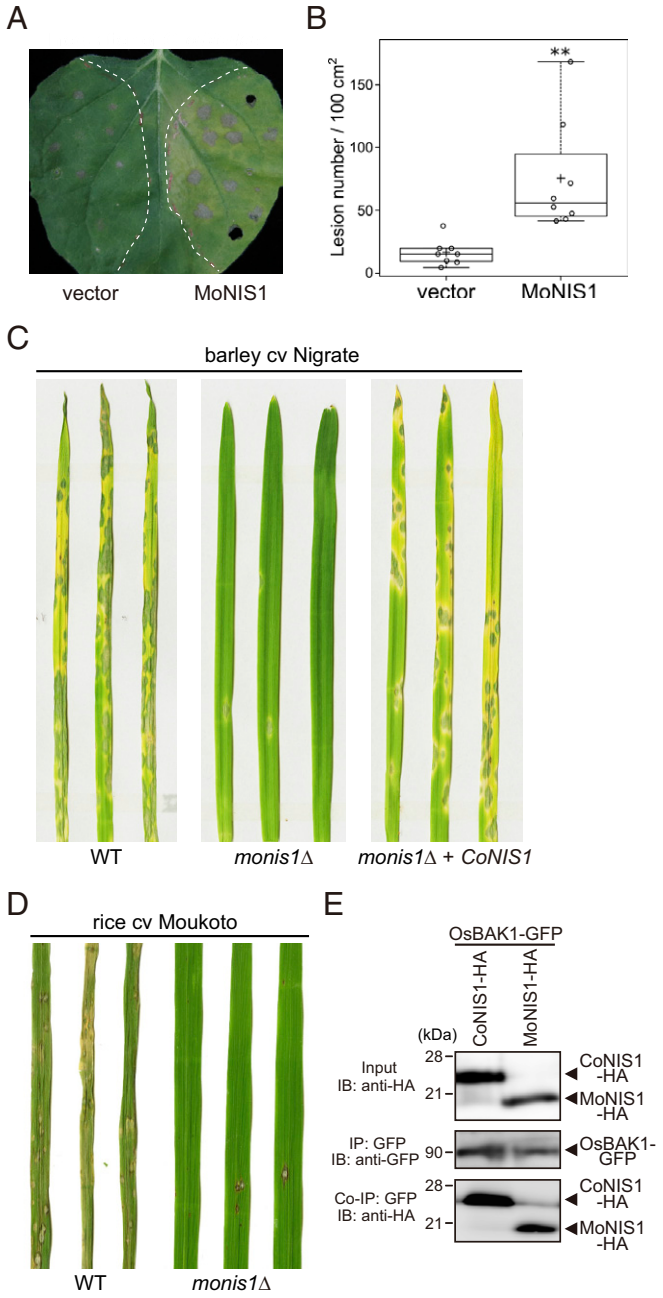

Fig. 7. NIS1 contributes to virulence of fungal pathogens. (*A*) Transient expression of MoNIS1 promotes lesion formation by *C. orbiculare* on *Nb*. Conidial suspensions (5×10^5 conidia per milliliter) of *C. orbiculare* wild-type strain were drop inoculated onto infiltration sites of *A. tumefaciens* harboring the plasmid expressing MoNIS1 or *A. tumefaciens* harboring the empty plasmid pBICP35 as a vector control (vector). Dashed lines represent the boundaries of infiltrated areas. The photograph was taken at 6 dpi. (*B*) Quantification of lesion number on *Nb* leaves transiently expressing MoNIS-HA after *C. orbiculare* inoculation. Conidial suspensions (5×10^5 conidia per milliliter) of *C. orbiculare* wild-type strain were spray inoculated onto infiltration sites of *A. tumefaciens* harboring a plasmid expressing MoNIS1 or of *A. tumefaciens* harboring the empty plasmid pBICP35 (vector). Lesion number for each infiltrated area was counted at 4 dpi. Center lines show the medians. Box limits indicate the 25th and 75th percentiles. Whiskers extend 1.5 times the interquartile range from the 25th and 75th percentiles. Crosses represent sample means. Data points are plotted as open circles; $n = 8$ biological replicates. The statistical significance of differences between means was determined by two-tailed *t* test. $^{**}P < 0.01$. (*C*) Inoculation assay of the *monis1*Δ mutant on barley (*H. vulgare* 'Nigrate'). Conidial suspensions of WT (Δ*ku70*), *monis1*Δ, and *monis1*Δ expressing *CoNIS1* genomic sequence were inoculated onto barley leaves, and incubated for 5 d. (*D*) Inoculation assay of the *monis1*Δ mutant on rice (*O. sativa* 'Moukoto'). Conidial suspensions of WT (Δ*ku70*) and *monis1*Δ were inoculated onto rice leaves and incubated for 7 d. (*E*) Co-IP of rice OsBAK1 and NIS1 homologs. OsBAK1-GFP was transiently coexpressed with CoNIS1-HA or MoNIS1-HA in *Nb*. Similar results were obtained from one additional experiment.

mali, a Sordariomycete fungus phylogenetically close to *M. oryzae*, carries two copies of *NIS1* homologs, one of which is closely related to *MoNIS1* while the other belongs to the same clade as *CoNIS1* (Fig. 1 and *SI Appendix*, Fig. S4), *M. oryzae* or a close ancestor species appears to have lost its *CoNIS1*-like *NIS1* homolog. The loss of this *NIS1* homolog might have enabled the pathogen to avoid recognition by a particular host plant while maintaining the essential ability to suppress host immunity by expressing the other *NIS1*.

Interestingly, it was recently reported that the expression of the *Fusarium virguliforme* NIS1 ortholog induced sudden death syndrome foliar symptoms in soybean, mimicking the development of soybean foliar symptoms caused by *F. virguliforme* itself in the field (49). Thus, NIS1-triggered cell death via plant recognition may be deployed by a pathogen for enhancing virulence in certain plant–fungal pathogen interactions. It is also noteworthy that the root endophyte fungus *C. tofieldiae* possesses a *NIS1* homolog (Fig. 1 and *SI Appendix*, Fig. S1), and this fungus exhibits high expression of the *NIS1* homolog during *Arabidopsis* colonization (25). We revealed that the *C. tofieldiae* NIS1 homolog suppresses flg22-triggered ROS generation in *Nb* in the same way as the pathogenic fungal NIS1s (Fig. 4 *A* and *G*). This suggests that *C. tofieldiae* uses NIS1 to colonize *Arabidopsis*, i.e., the endophyte fungus needs effectors, including NIS1, to establish its beneficial interaction with *Arabidopsis*.

Expression of CoNIS1 and its orthologs in *Nb* almost completely abolishes flg22-triggered ROS generation (Fig. 4*A*). We found that NIS1 interacts with BIK1, resulting in the inhibition of the BIK1-RBOHD interaction (Fig. 4 *C* and *E*). BIK1 induces flg22-triggered ROS generation by phosphorylating RBOHD in *Arabidopsis*. *Arabidopsis* RBOHD shares high similarity with NbRbohB (50) and complements the loss of the flg22-induced ROS burst in *NbRbohB*-silenced *Nb* plants (9), indicating that NbRbohB is a functional ortholog of *Arabidopsis* RBOHD. Although a functional ortholog of BIK1 has not yet been identified in *Nb*, we propose that NIS1 targets such an ortholog, inhibiting the PAMP-triggered ROS generation that largely depends on NbRbohB (51).

BIK1 is a key component that links PTI signals from transmembrane PAMP receptor complexes to intracellular immune responses, although it is unclear how BIK1 regulates downstream signaling except for the direct activation of RBOHD (9, 10). The *rbohb*-silenced *Nb* displayed reduced ROS production and decreased resistance to *P. infestans* (52). However, *rbohb* silencing did not reduce the immunity of *Nb* to *C. orbiculare* (53), whereas the expression of NIS1 in *Nb* enhanced susceptibility to *C. orbiculare* (Fig. 7 *A* and *B*). This indicates that inhibition of PAMP-triggered ROS generation is insufficient to reduce *Nb* immunity to *C. orbiculare*. Consistent with this, both *Arabidopsis rbohD* and *rbohF* mutants maintain immunity to *C. tropicale* (39), but in contrast the *Arabidopsis bik1* mutant as well as the *bak1-5* mutant display reduced immunity to the same pathogen (Fig. 6 *C* and *D*). It is necessary to investigate further the plant defense pathways that are effective against *Colletotrichum* fungi, which partially depend on BAK1 and its related RLKs as well as BIK1 and may be dampened by NIS1. We also showed that MoNIS1 suppressed R3a/Avr3a-dependent HR cell death in *Nb* (*SI Appendix*, Fig. S8), which is not suppressed in *serk3*-silenced *Nb* (36). Thus, NIS1 may have additional targets, probably belonging to a kinase family that regulates R3a/Avr3a-triggered ETI.

Deletion of the *NIS1* ortholog *MoNIS1* severely compromised the virulence of *M. oryzae* on rice and barley (Fig. 7 *C* and *D*). OsBAK1 is reportedly involved in rice immunity to *M. oryzae* (41). Taken together with the interaction of CoNIS1 and MoNIS1 with OsBAK1 (Fig. 7*E*), this result implies that *M. oryzae* needs to suppress OsBAK1 function via MoNIS1 for successful infection. Also, it was reported that a rice RLCK named OsRLCK185 is involved in rice immunity and targeted by the bacterial effector Xoo1488 (54). MoNIS1 may target RLCKs, including OsRLCK185, of rice and/or barley to enhance the virulence of *M. oryzae* toward these species.

Materials and Methods

Plasmids were constructed as described in detail in *SI Appendix, SI Materials and Methods* and Table S3. Methods for plant growth, yeast two-hybrid assay, ROS measurement, in vitro kinase activity assay, and colocalization assay are also described in detail in *SI Appendix, SI Materials and Methods*.

Fungal Strains and Media. The *C. orbiculare* (syn. *Colletotrichum lagenarium*) wild-type strain 104-T (MAFF240422) is stored at the Laboratory of Plant Pathology, Kyoto University. *C. tropicale* (previously reported as *C. gloeosporioides*) S9275 (MAFF840071) was provided by Shigenobu Yoshida, National Institute for Agro-Environmental Sciences, Ibaraki, Japan. *C. higginsianum* MAFF305635 was obtained from National Agriculture and Food Research Organization, GenBank, Ibaraki, Japan. Cultures of all fungal isolates of *Colletotrichum* were maintained on 3.9% (wt/vol) PDA medium (BD Difco) at 24 °C in the dark. For conidiation, a *C. tropicale* culture was placed in a cycle of 16 h black light and 8 h dark. All strains of *M. oryzae* used in this study are stored at the Iwate Biotechnology Research Center. The Δ*ku70* mutant of *M. oryzae* strain Guy11 (55), provided by N. J. Talbot, University of Exeter, Devon, UK, was used as the wild-type strain. Cultures of *M. oryzae* were maintained on oatmeal agar medium at 25 °C in the dark. For conidiation, a *M. oryzae* culture was grown under a black light (FS20S/BLB 20W, Toshiba) for 4 d at 22 °C, after aerial hyphae of the colonies had been washed away with sterilized distilled water.

Transient Expression in *Nb*. *Nb* plants (5–6 wk old) were used for agroinfiltration assays. Constructs derived from pBICP35 were used to transform *Agrobacterium tumefaciens* GV3101 (56) by electroporation. Transformant cells were cultured and harvested by centrifugation and suspended in MMA induction buffer (1 L MMA: 5 g MS salts, 1.95 g Mes, 20 g sucrose, 200 mM acetosyringone, pH 5.6). The suspensions were infiltrated into *Nb* leaves using a syringe. For cell death suppression assay, at 1 d after infiltration with *A. tumefaciens* carrying a plasmid harboring each *NIS1* homolog, the infiltration site was challenged with a recombinant *A. tumefaciens* strain carrying a plasmid harboring *INF1* or a mixture of two *A. tumefaciens* strains carrying plasmids harboring either $Avr3a^{KI}$ (Δ23–147) or *R3a*. All suspensions were incubated for 1 h before infiltration. INF1-induced cell death was observed at 3 dpi. Protein extracts were analyzed by immunoblot using anti-HA (3F10, Roche), anti-GFP [GFP(B-2), Santa Cruz Biotechnology] and anti-FLAG (F-3165, Sigma-Aldrich) antibodies. HRP-linked anti-rat (7077, Cell Signaling Technology) and anti-mouse (7076, Cell Signaling Technology) IgG were used as secondary antibodies.

Coimmunoprecipitation Assays. Microsomal fractions were extracted from agroinfiltrated *Nb* leaves at 2 dpi by homogenizing with extraction buffer [50 mM Tris·HCl pH 7.4, 150 mM NaCl, 5% glycerol, 0.5% Triton X-100, protease inhibitor mixture (11836153001, Roche)] on ice. Crude protein extracts were centrifuged at 20,000 × *g* for 10 min to remove cell debris, and the supernatants were then incubated with μMACS anti-GFP magnetic microbeads (130-091-288, Miltenyi Biotec) for 1 h at 4 °C with gentle rotation. For MoNIS1-BIK1 interaction, the supernatants were incubated with GFP-trap-A (ChromoTek) for 2 h at 4 °C. After three washing steps with wash buffer (50 mM Tris·HCl pH 7.4, 150 mM NaCl, 5% glycerol, 0.1% Triton X-100), immunoprecipitates were analyzed by immunoblotting with anti-HA (3F10, Roche), anti-GFP [GFP(B-2), Santa Cruz Biotecnology] and anti-FLAG (F-3165, Sigma-Aldrich) antibodies. HRP-linked anti-rat (7077, Cell Signaling Technology) and anti-mouse (7076, Cell Signaling Technology) IgG were used as secondary antibodies.

Pathogen Inoculation Assays. In an inoculation assay of *C. orbiculare* on *Nb*, 2 d after infiltration with *A. tumefaciens* carrying a plasmid harboring MoNIS1-HA or pBICP35 (empty vector), 10 μL of a conidial suspension (5×10^5 conidia per milliliter) of *C. orbiculare* 104-T strain was drop inoculated (for lesion size evaluation) or spray inoculated (for lesion number quantification) onto the infiltration areas of detached leaves. After incubation for 4 d at 24 °C, the lesion number of each infiltrated area was measured. Mean and SD were calculated for "lesion number per 100 cm^2" values from eight independent infiltration areas. The statistical significance of differences between means was determined by unpaired *t* test (two tailed). Statistical significance was defined as a *P* value of 0.01 or lower. An inoculation assay of adapted *C. higginsianum* on *Arabidopsis* mutants was performed as follows: A conidial suspension of *C. higginsianum* (2.5×10^5 conidia per milliliter) was inoculated onto leaves of *Arabidopsis* WT (Col-0), *bak1-5*, *bik1-1*, and *bik1-1 pbl1-1* plants and incubated for 5 d. The lesion diameter of inoculated leaves was determined with Adobe Photoshop. At least 50 lesions were measured in each experiment. Mean and SD were calculated from three independent experiments. The statistical significance of differences between means was determined by unpaired *t* test (two tailed); statistical significance was defined as a *P* value of 0.05 or lower. To measure entry (invasion) rates, conidia (5×10^5 conidia per milliliter) of the pathogen were inoculated on cotyledons, which were then mounted in water under a coverslip, with the inoculated surface facing the objective lens. The invasion ratio (%) was calculated by the following numerical formula: (number of appressoria forming invasive hyphae)/(number of appressoria) × 100. One hundred appressoria were observed at 3 dpi on each plant. Mean and SD were calculated from five independent plant samples. The statistical significance of differences between means was determined by unpaired *t* test (two tailed), with statistical significance defined as a *P* value of 0.01 or lower. An inoculation assay of nonadapted *C. tropicale* on *Arabidopsis* mutants was performed as follows: A conidial suspension of *C. tropicale* (5×10^5 conidia per milliliter) with 0.1% glucose was inoculated onto leaves of *Arabidopsis* WT (Col-0), *pen2-1*, *bak1-5*, *bik1-1*, and *bik1-1 pbl1-1* plants and incubated for 4 d. To measure entry (invasion) rates, the pathogen was inoculated with 0.05% glucose on cotyledons and the invasion ratio (%) was calculated by the following numerical formula: (number of conidia forming invasive hyphae)/(number of germinating conidia) × 100. At least 100 conidia were observed at ∼14 hpi in each experiment. Means and SD were calculated from three independent experiments. The statistical significance of differences between means was determined by unpaired *t* test (two tailed). Statistical significance was defined as a *P* value of 0.01 or lower. For an inoculation assay of *M. oryzae* on barley and rice, a conidial suspension of *M. oryzae* (5×10^4 conidia per milliliter) containing 0.01% Tween 20 was sprayed onto susceptible barley cotyledons (*Hordeum vulgare* 'Nigrate') and rice seedlings (*Oryza sativa* 'Moukoto') of the fourth leaf stage. Inoculated plants were placed in a dew chamber at 27 °C for 24 h in the dark and then transferred to a growth chamber with a photoperiod of 16 h.

***MoNIS1* Gene Disruption and Complementation in *M. oryzae*.** To obtain protoplasts, hyphae of *M. oryzae* strains were incubated for 3 d in 200 mL of YG medium (5 g of yeast extract, and 20 g of glucose per liter). Protoplast preparation and transformation were performed as described previously (57). Hygromycin- or bialaphos-resistant transformants were selected on plates with 300 μg/mL of hygromycin B (Wako Pure Chemicals) or 250 μg/mL of bialaphos (Wako Pure Chemicals), respectively. Targeted gene disruption of *MoNIS1* in *M. oryzae* was performed by homologous recombination using a gene disruption vector. The primers used for generating the vector are listed in *SI Appendix*, Table S3. Transformants were analyzed by PCR with the primers MoNIS1F/MoNIS1R, with *HPH*-specific primers, or with bialaphos resistance gene (*bar*)-specific primers.

Phylogenetic Analysis. We used ETE Toolkit version 3.0.0b35 (58) to construct a maximum likelihood tree of NIS1 homologs. Multiple alignment of protein sequences of NIS1 homologs was generated with Clustal Omega version 1.2.1 (59). Alignment cleaning was performed by trimAl v1.4 (60) with "–gt 0.1" setting. A maximum likelihood tree was obtained using PhyML version 20131022 (61) with the JTT model and 100 bootstrap replicates. Species tree topologies were built with CVTree version 5.0 (62, 63) using the predicted proteomes of 141 fungal species (*SI Appendix*, Table S2). The final NIS1 protein tree was reconstructed using Treefix-DTL version 1.0.2 (64) with the above-generated NIS1 protein alignments (*SI Appendix*, Fig. S1), NIS1 ML tree (*SI Appendix*, Fig. S4) and species tree (*SI Appendix*, Fig. S4) as inputs. Trees were visualized using iTOL (ref. 65; https://itol.embl.de/).

ACKNOWLEDGMENTS. We thank Sophien Kamoun (The Sainsbury Laboratory) for $pGR106\text{-}AVR3a^{KI}$ (Δ23–147) and p35S-INF1; Hirofumi Yoshioka (Nagoya University) for pBinPlus-R3a; Yasuhiro Kadota (RIKEN, CSRS) for *bik1*, *bik1 pbl1*, and chitin; Kei Hiruma (Nara Institute of Science and Technology) for *C. tofieldiae* cDNA; Nick Talbot (University of Exeter) for the

Δ*ku70* line of *M. oryzae* Guy11; and Kyoko Ikeda, Kae Yoshino, and Kiwamu Hyodo for technical assistance. This work was supported by the Leading Initiative for Excellent Young Researchers program of the Ministry of Education, Culture, Sports, Science, and Technology; by Grants-in-Aid for Scientific Research (15H05780, 18H02204, 18H04780, and 18K19212); by grants from the Project of the NARO Bio-oriented Technology Research Advancement Institution (Research program on development of innovative technology); and by the Asahi Glass Foundation.

1. Monaghan J, Zipfel C (2012) Plant pattern recognition receptor complexes at the plasma membrane. *Curr Opin Plant Biol* 15:349–357.
2. Chinchilla D, et al. (2007) A flagellin-induced complex of the receptor FLS2 and BAK1 initiates plant defence. *Nature* 448:497–500.
3. Heese A, et al. (2007) The receptor-like kinase SERK3/BAK1 is a central regulator of innate immunity in plants. *Proc Natl Acad Sci USA* 104:12217–12222.
4. Lu D, et al. (2010) A receptor-like cytoplasmic kinase, BIK1, associates with a flagellin receptor complex to initiate plant innate immunity. *Proc Natl Acad Sci USA* 107: 496–501.
5. Zhang J, et al. (2010) Receptor-like cytoplasmic kinases integrate signaling from multiple plant immune receptors and are targeted by a *Pseudomonas syringae* effector. *Cell Host Microbe* 7:290–301.
6. Roux M, et al. (2011) The *Arabidopsis* leucine-rich repeat receptor-like kinases BAK1/SERK3 and BKK1/SERK4 are required for innate immunity to hemibiotrophic and biotrophic pathogens. *Plant Cell* 23:2440–2455.
7. Sun Y, et al. (2013) Structural basis for flg22-induced activation of the *Arabidopsis* FLS2-BAK1 immune complex. *Science* 342:624–628.
8. Couto D, Zipfel C (2016) Regulation of pattern recognition receptor signalling in plants. *Nat Rev Immunol* 16:537–552.
9. Kadota Y, et al. (2014) Direct regulation of the NADPH oxidase RBOHD by the PRR-associated kinase BIK1 during plant immunity. *Mol Cell* 54:43–55.
10. Li L, et al. (2014) The FLS2-associated kinase BIK1 directly phosphorylates the NADPH oxidase RbohD to control plant immunity. *Cell Host Microbe* 15:329–338.
11. Shan L, et al. (2008) Bacterial effectors target the common signaling partner BAK1 to disrupt multiple MAMP receptor-signaling complexes and impede plant immunity. *Cell Host Microbe* 4:17–27.
12. Yamaguchi K, et al. (2013) Suppression of rice immunity by *Xanthomonas oryzae* type III effector Xoo2875. *Biosci Biotechnol Biochem* 77:796–801.
13. Zhou J, et al. (2014) The *Pseudomonas syringae* effector HopF2 suppresses *Arabidopsis* immunity by targeting BAK1. *Plant J* 77:235–245.
14. Li L, et al. (2016) Activation-dependent destruction of a co-receptor by a *Pseudomonas syringae* effector dampens plant immunity. *Cell Host Microbe* 20:504–514.
15. Feng F, et al. (2012) A *Xanthomonas* uridine 5′-monophosphate transferase inhibits plant immune kinases. *Nature* 485:114–118.
16. Rooney HC, et al. (2005) Cladosporium Avr2 inhibits tomato Rcr3 protease required for *Cf-2*-dependent disease resistance. *Science* 308:1783–1786.
17. Song J, et al. (2009) Apoplastic effectors secreted by two unrelated eukaryotic plant pathogens target the tomato defense protease Rcr3. *Proc Natl Acad Sci USA* 106: 1654–1659.
18. Bos JI, et al. (2010) *Phytophthora infestans* effector AVR3a is essential for virulence and manipulates plant immunity by stabilizing host E3 ligase CMPG1. *Proc Natl Acad Sci USA* 107:9909–9914.
19. Dagdas YF, et al. (2016) An effector of the Irish potato famine pathogen antagonizes a host autophagy cargo receptor. *eLife* 5:e10856.
20. de Jonge R, et al. (2010) Conserved fungal LysM effector Ecp6 prevents chitin-triggered immunity in plants. *Science* 329:953–955.
21. Mentlak TA, et al. (2012) Effector-mediated suppression of chitin-triggered immunity by *magnaporthe oryzae* is necessary for rice blast disease. *Plant Cell* 24:322–335.
22. Bart R, et al. (2012) High-throughput genomic sequencing of cassava bacterial blight strains identifies conserved effectors to target for durable resistance. *Proc Natl Acad Sci USA* 109:E1972–E1979.
23. Yoshino K, et al. (2012) Cell death of *Nicotiana benthamiana* is induced by secreted protein NIS1 of *Colletotrichum orbiculare* and is suppressed by a homologue of CgDN3. *Mol Plant Microbe Interact* 25:625–636.
24. Shen S, Goodwin PH, Hsiang T (2001) Infection of *Nicotiana* species by the anthracnose fungus, *Colletotrichum orbiculare*. *Eur J Plant Pathol* 107:767–773.
25. Hiruma K, et al. (2016) Root endophyte *Colletotrichum tofieldiae* confers plant fitness benefits that are phosphate status dependent. *Cell* 165:464–474.
26. Kamoun S, et al. (1997) A gene encoding a protein elicitor of *Phytophthora infestans* is down-regulated during infection of potato. *Mol Plant Microbe Interact* 10:13–20.
27. Vleeshouwers VG, et al. (2006) Agroinfection-based high-throughput screening reveals specific recognition of INF elicitins in *Solanum*. *Mol Plant Pathol* 7:499–510.
28. Cheng Y, et al. (2017) PSTha5a23, a candidate effector from the obligate biotrophic pathogen *Puccinia striiformis* f. sp. *tritici*, is involved in plant defense suppression and rust pathogenicity. *Environ Microbiol* 19:1717–1729.
29. Xie J, et al. (2016) A novel *Meloidogyne incognita* effector Misp12 suppresses plant defense response at latter stages of nematode parasitism. *Front Plant Sci* 7:964.
30. Bos JI, et al. (2006) The C-terminal half of *Phytophthora infestans* RXLR effector AVR3a is sufficient to trigger R3a-mediated hypersensitivity and suppress INF1-induced cell death in *Nicotiana benthamiana*. *Plant J* 48:165–176.
31. Chaparro-Garcia A, et al. (2011) The receptor-like kinase SERK3/BAK1 is required for basal resistance against the late blight pathogen *phytophthora infestans* in *Nicotiana benthamiana*. *PLoS One* 6:e16608.
32. Du J, et al. (2015) Elicitin recognition confers enhanced resistance to *Phytophthora infestans* in potato. *Nat Plants* 1:15034.
33. Irieda H, et al. (2014) *Colletotrichum orbiculare* secretes virulence effectors to a biotrophic interface at the primary hyphal neck via exocytosis coupled with SEC22-mediated traffic. *Plant Cell* 26:2265–2281.
34. Khang CH, et al. (2010) Translocation of *Magnaporthe oryzae* effectors into rice cells and their subsequent cell-to-cell movement. *Plant Cell* 22:1388–1403.
35. Giraldo MC, et al. (2013) Two distinct secretion systems facilitate tissue invasion by the rice blast fungus *Magnaporthe oryzae*. *Nat Commun* 4:1996.
36. Ma Z, et al. (2015) A *Phytophthora sojae* glycoside hydrolase 12 protein is a major virulence factor during soybean infection and is recognized as a PAMP. *Plant Cell* 27: 2057–2072.
37. Macho AP, Zipfel C (2014) Plant PRRs and the activation of innate immune signaling. *Mol Cell* 54:263–272.
38. Schwessinger B, et al. (2011) Phosphorylation-dependent differential regulation of plant growth, cell death, and innate immunity by the regulatory receptor-like kinase BAK1. *PLoS Genet* 7:e1002046.
39. Hiruma K, et al. (2011) *Arabidopsis ENHANCED DISEASE RESISTANCE 1* is required for pathogen-induced expression of plant defensins in nonhost resistance, and acts through interference of *MYC2*-mediated repressor function. *Plant J* 67:980–992.
40. Lipka V, et al. (2005) Pre- and postinvasion defenses both contribute to nonhost resistance in *Arabidopsis*. *Science* 310:1180–1183.
41. Park HS, et al. (2011) A subset of *OsSERK* genes, including *OsBAK1*, affects normal growth and leaf development of rice. *Mol Cells* 32:561–569.
42. Doehlemann G, et al. (2009) Pep1, a secreted effector protein of *Ustilago maydis*, is required for successful invasion of plant cells. *PLoS Pathog* 5:e1000290.
43. Hemetsberger C, et al. (2015) The fungal core effector Pep1 is conserved across smuts of dicots and monocots. *New Phytol* 206:1116–1126.
44. Bressendorff S, et al. (2016) An innate immunity pathway in the moss *Physcomitrella patens*. *Plant Cell* 28:1328–1342.
45. Mukhtar MS, et al.; European Union Effectoromics Consortium (2011) Independently evolved virulence effectors converge onto hubs in a plant immune system network. *Science* 333:596–601.
46. Lozano-Torres JL, et al. (2012) Dual disease resistance mediated by the immune receptor Cf-2 in tomato requires a common virulence target of a fungus and a nematode. *Proc Natl Acad Sci USA* 109:10119–10124.
47. Roux B, et al. (2015) Genomics and transcriptomics of *Xanthomonas campestris* species challenge the concept of core type III effectome. *BMC Genomics* 16:975.
48. Gan P, et al. (2013) Comparative genomic and transcriptomic analyses reveal the hemibiotrophic stage shift of *Colletotrichum* fungi. *New Phytol* 197:1236–1249.
49. Chang HX, et al. (2016) Identification of multiple phytotoxins produced by *Fusarium virguliforme* including a phytotoxic effector (FvNIS1) associated with sudden death syndrome foliar symptoms. *Mol Plant Microbe Interact* 29:96–108.
50. Kobayashi M, et al. (2007) Calcium-dependent protein kinases regulate the production of reactive oxygen species by potato NADPH oxidase. *Plant Cell* 19:1065–1080.
51. Segonzac C, et al. (2011) Hierarchy and roles of pathogen-associated molecular pattern-induced responses in *Nicotiana benthamiana*. *Plant Physiol* 156:687–699.
52. Yoshioka H, et al. (2003) *Nicotiana benthamiana* gp91^{phox} homologs *NbrbohA* and *NbrbohB* participate in H_2O_2 accumulation and resistance to *Phytophthora infestans*. *Plant Cell* 15:706–718.
53. Asai S, Ohta K, Yoshioka H (2008) MAPK signaling regulates nitric oxide and NADPH oxidase-dependent oxidative bursts in *Nicotiana benthamiana*. *Plant Cell* 20:1390–1406.
54. Yamaguchi K, et al. (2013b) A receptor-like cytoplasmic kinase targeted by a plant pathogen effector is directly phosphorylated by the chitin receptor and mediates rice immunity. *Cell Host Microbe* 13:347–357.
55. Kershaw MJ, Talbot NJ (2009) Genome-wide functional analysis reveals that infection-associated fungal autophagy is necessary for rice blast disease. *Proc Natl Acad Sci USA* 106:15967–15972.
56. Koncz C, Schell J (1986) The promoter of T_L-DNA gene 5 controls the tissue-specific expression of chimaeric genes carried by a novel type of *Agrobacterium* binary vector. *Mol Gen Genet* 204:383–396.
57. Takano Y, Komeda K, Kojima K, Okuno T (2001) Proper regulation of cyclic AMP-dependent protein kinase is required for growth, conidiation, and appressorium function in the anthracnose fungus *Colletotrichum lagenarium*. *Mol Plant Microbe Interact* 14:1149–1157.
58. Huerta-Cepas J, Serra F, Bork P (2016) ETE 3: Reconstruction, analysis, and visualization of phylogenomic data. *Mol Biol Evol* 33:1635–1638.
59. Sievers F, et al. (2011) Fast, scalable generation of high-quality protein multiple sequence alignments using Clustal Omega. *Mol Syst Biol* 7:539.
60. Capella-Gutiérrez S, Silla-Martínez JM, Gabaldón T (2009) trimAl: A tool for automated alignment trimming in large-scale phylogenetic analyses. *Bioinformatics* 25: 1972–1973.
61. Guindon S, et al. (2010) New algorithms and methods to estimate maximum-likelihood phylogenies: Assessing the performance of PhyML 3.0. *Syst Biol* 59:307–321.
62. Qi J, Wang B, Hao BI (2004) Whole proteome prokaryote phylogeny without sequence alignment: A K-string composition approach. *J Mol Evol* 58:1–11.
63. Zuo G, Hao B (2015) CVTree3 web server for whole-genome-based and alignment-free prokaryotic phylogeny and taxonomy. *Genomics Proteomics Bioinformatics* 13: 321–331.
64. Bansal MS, Wu YC, Alm EJ, Kellis M (2015) Improved gene tree error correction in the presence of horizontal gene transfer. *Bioinformatics* 31:1211–1218.
65. Letunic I, Bork P (2016) Interactive tree of life (iTOL) v3: An online tool for the display and annotation of phylogenetic and other trees. *Nucleic Acids Res* 44:W242–W245.